THE JOURNAL OF BIOLOGICAL CHEMISTRY VOL. 291, NO. 20, pp. 10759–10771, May 13, 2016

The N-terminal Part of *Arabidopsis thaliana* Starch Synthase 4 Determines the Localization and Activity of the Enzyme*[S]

Received for publication, October 14, 2015, and in revised form, March 11, 2016 Published, JBC Papers in Press, March 11, 2016, DOI 10.1074/jbc.M115.698332

Sandy Raynaud, Paula Ragel, Tomás Rojas, and Ángel Mérida[1]

From the Instituto de Bioquímica Vegetal y Fotosíntesis, Consejo Superior de Investigaciones Científicas, University of Sevilla, Avenida Américo Vespucio 49, 41092 Sevilla, Spain

Starch synthase 4 (SS4) plays a specific role in starch synthesis because it controls the number of starch granules synthesized in the chloroplast and is involved in the initiation of the starch granule. We showed previously that SS4 interacts with fibrillins 1 and is associated with plastoglobules, suborganelle compartments physically attached to the thylakoid membrane in chloroplasts. Both SS4 localization and its interaction with fibrillins 1 were mediated by the N-terminal part of SS4. Here we show that the coiled-coil region within the N-terminal portion of SS4 is involved in both processes. Elimination of this region prevents SS4 from binding to fibrillins 1 and alters SS4 localization in the chloroplast. We also show that SS4 forms dimers, which depends on a region located between the coiled-coil region and the glycosyltransferase domain of SS4. This region is highly conserved between all SS4 enzymes sequenced to date. We show that the dimerization seems to be necessary for the activity of the enzyme. Both dimerization and the functionality of the coiled-coil region are conserved among SS4 proteins from phylogenetically distant species, such as *Arabidopsis* and *Brachypodium*. This finding suggests that the mechanism of action of SS4 is conserved among different plant species.

Starch plays an essential role in the metabolism of photosynthetic organisms. Starch accumulates in the chloroplast during the day as a final step in photosynthetic carbon assimilation. This transitory starch is mobilized during the night to fulfil the metabolic requirements of the plant in the absence of photosynthesis (1). In addition, the starch is stored long-term in the storage organs of some species, such as seed endosperm or tubers, and provides carbon skeletons and energy to support some phases of growth, such as germination or sprouting processes (2). Over the last few years, intense interest in starch has led to the characterization of many of the elements known in this pathway (2, 3) and the discovery of new elements (4). An important activity in starch synthesis is elongation, which is carried out by the starch synthases (SSs)[2] (glycosyl-transferring, EC 2.4.1.21). The SSs catalyze the transfer of the glucosyl moiety in ADP-glucose to the nonreducing end of a pre-existing α-1,4 glucan primer (5). Five SS classes are found in all organisms that synthesize starch: SS1, SS2, SS3, SS4, and granule-bound starch synthase I. The SSs harbor a region that is highly conserved within glycogen synthases (GSs). This region corresponds to the C terminus of plant SSs and includes the starch catalytic domain (Pfam PF08323) and the glycosyltransferase 1 domain (Pfam PF00534) characteristic of the GT5 glycosyltransferase superfamily (6) and described as glycosyltransferases with the glycosyltransferase-B structural fold by the Carbohydrate Active Enzyme Database. In contrast, the N-terminal region carries a sequence specific for each SS, varying both in size and amino acid sequence. This region is absent from GSs. The N-terminal region of SSs does not seem to be involved in catalysis, but it may alter some of the catalytic properties of these enzymes (7, 8).

Our group showed previously that SS4 is involved in a process that has not been well characterized: the initiation of the starch granule (9). SS4 controls the number of starch granules synthesized in the chloroplast. Its elimination determines the accumulation of only one (or in some cases two) granules/chloroplasts (9, 10). We also found that the hilum (starch granule core) of the starch granules synthesized in plants that lack SS4 activity is different from the hilum observed in WT plants. This difference indicates that SS4 participates in the formation of the primer required for the *de novo* synthesis of a starch granule (10). Recently, we showed that SS4 is not present in soluble form in the plastidial stroma. Instead, it is associated with the thylakoid membranes. SS4 interacts with fibrillins 1a and 1b (FBN1) proteins and seems to be associated with plastoglobules close and physically attached to thylakoids. Both this localization and the interaction with the fibrillins are mediated by the N-terminal portion of SS4 (11). As mentioned above, the N-terminal part of SS4 is specific to this class of SSs. It is a long segment, containing 543 amino acids in the case of *Arabidopsis* SS4 (At4g18240), and is well conserved among all of the SS4 proteins from different species sequenced to date. The main feature of the SS4 N terminus is the presence of a long coiled-coil region (9).

In this study, we analyzed the function of the different domains present in the N-terminal part of SS4. We show that

* This work was funded by grants BIO2012–35043 from the Secretaría de Estado de Investigación, Desarrollo e Innovación and BIO1180 from the Consejería de Economía, Innovación, Ciencia y Empleo, Junta de Andalucía and the European Union-FEDER. The authors declare that they have no conflicts of interest with the contents of this article.

[S] This article contains supplemental Table S1.

[1] To whom correspondence should be addressed: Instituto de Bioquímica Vegetal y Fotosíntesis, CSIC-US, Avda. Américo Vespucio 49, 41092 Sevilla, Spain. Tel.: 34-954-489-507; E-mail: angel.merida@csic.es.

[2] The abbreviations used are: SS, starch synthase; GS, glycogen synthase; CFP, cyan fluorescent protein; BiFC, bimolecular fluorescence complementation; CTP, chloroplast transit peptide; CR, conserved region; WOCR, without conserved region; Tricine, *N*-[2-hydroxy-1,1-bis(hydroxymethyl)ethyl]-glycine.

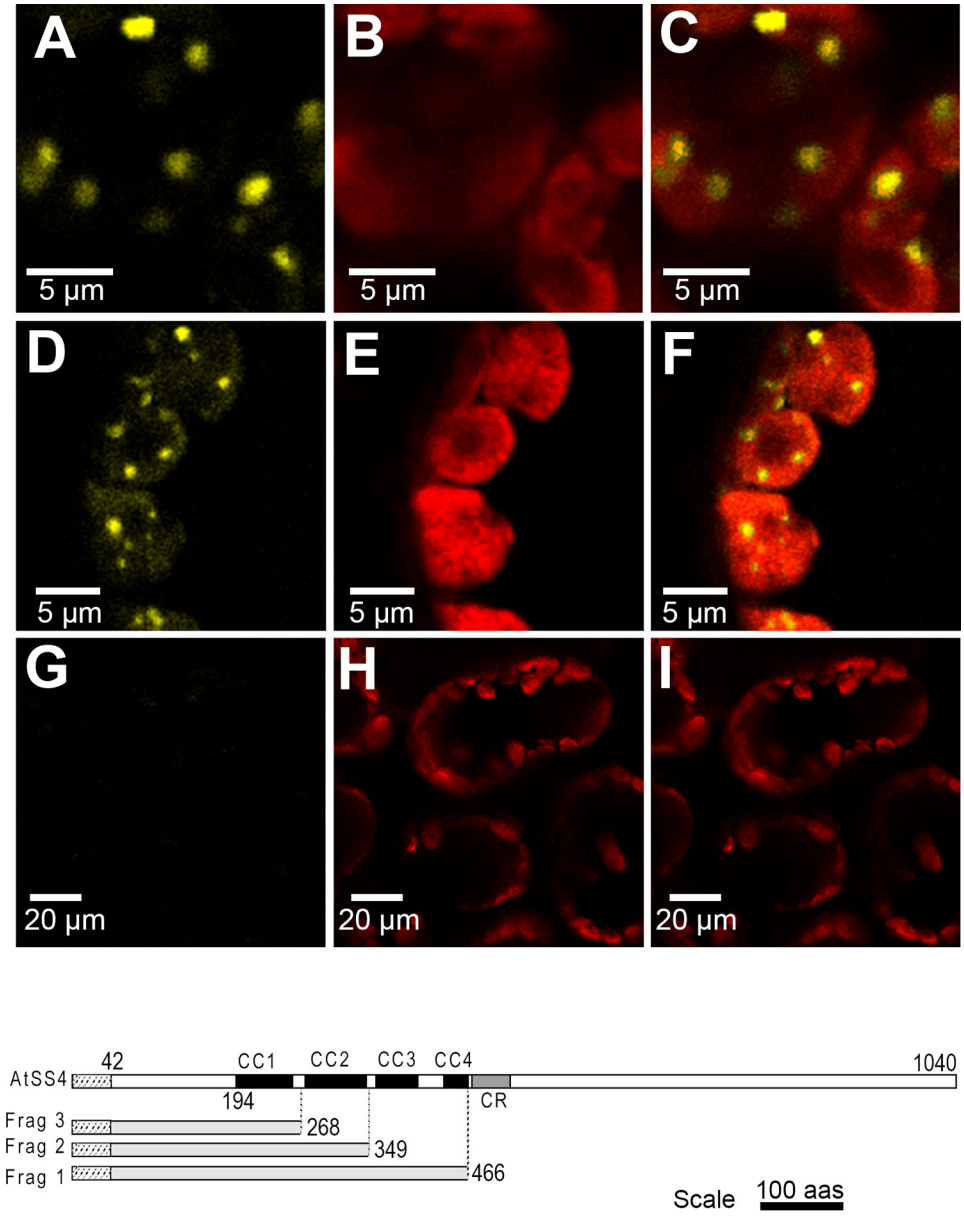

FIGURE 1. **Interaction of different SS4 fragments with FBN1b.** *Top panels*, fluorescence images showing YFP/CFP fluorescence signals from labeled proteins (*left panels*, *yellow*), chlorophyll autofluorescence (*center panels*, *red*), and merged images of proteins and chlorophyll in *N. benthamiana* leaves (*right panels*). The leaves were co-transformed with a cDNA encoding FBN1b fused to the C-terminal moiety of the CFP sequence and a cDNA encoding the *Arabidopsis* SS4 fragment 1 (*A–C*), fragment 2 (*D–F*), or fragment 3 (*G–I*) fused to the N-terminal half of the YFP sequence. The *yellow* signal indicates an interaction between FBN1b and the SS4 fragment. *Bottom panel*, schematic showing the *Arabidopsis* SS4 protein and the positions of fragments (*Frag*) 1, 2, and 3 in the protein. *Black boxes* correspond to coiled-coil regions. The *gray box* indicates the highly conserved region found in SS4 proteins. The *dotted box* indicates the CTP of the SS4 protein. The numbers indicate the positions of the respective amino acid residues (*aas*).

the coiled-coil region of the protein is necessary for the interaction with the FBN1 protein and the localization of SS4. We also show that SS4 forms a dimer *in vivo*. The interaction between SS4 monomers occurs via a region distinct from the coiled-coil domains that is highly conserved among the SS4 proteins of different species. We discuss the potential implications of SS4 dimerization in starch metabolism.

Experimental Procedures

Plant Materials—Nicotiana benthamiana plants were grown in soil pots in a greenhouse under a 16-h light/8-h dark cycle at 22 °C and 250 micro-Einsteins m^{-2} s^{-1} light intensity. *Arabidopsis thaliana* WT ecotype Col-0, *ss4*-1 mutant (9) and *ss4*-1 transgenic lines were sown in soil pots and grown in growth cabinets under a 16-h light/8-h dark photoregime, 23 °C (day)/20 °C (night), 70% humidity, and 120 micro-Einsteins m^{-2} s^{-1} light intensity (at the plant levels) supplied with white fluorescent lamps.

Plasmids Construction—The cDNAs used for transitory expression of the different truncated versions of the AtSS4 protein in *N. benthamiana* were cloned using the Gateway system (Invitrogen). The different fragments were amplified using the oligonucleotides shown in supplemental Table S1. The sequenced fragments were cloned into the pDONR207

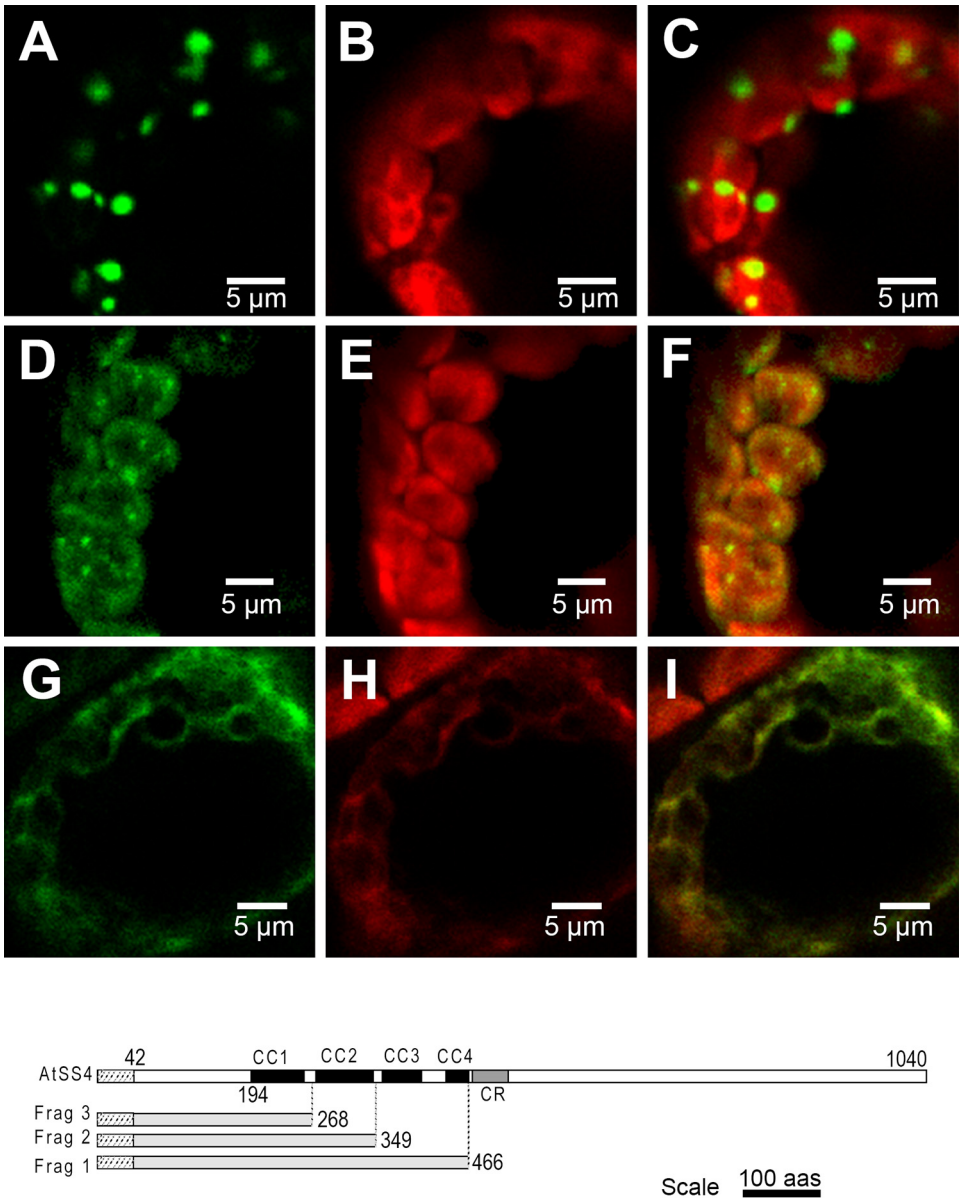

FIGURE 2. **Localization of different SS4 fragments fused to GFP in *N. benthamiana* chloroplasts.** *Top panels*, fluorescence images showing GFP fluorescence (*left panels*, *green*), chlorophyll autofluorescence (*center panels*, *red*), and merged images of proteins and chlorophyll (*right panels*) in *N. benthamiana* leaves. The leaves were transiently transformed with a cDNA encoding SS4 fragment 1 (*A–C*), fragment 2 (*D–E*), or fragment 3 (*G–I*) fused to a GFP sequence. *Bottom panel*, schematic showing the *Arabidopsis* SS4 protein and the positions of fragments (*Frag*) 1, 2, and 3 in the protein. *Black boxes* correspond to coiled-coil regions. The *gray box* indicates the highly conserved region found in SS4 proteins. The *dotted box* indicates the CTP of the SS4 protein. The numbers indicate the positions of the respective amino acid residues (*aas*).

plasmid (Invitrogen) via a BP clonase reaction. The stop codon was eliminated to allow C terminus translational fusion of the fragment with GFP (pEarleyGate 103) (12) for protein localization. Similar translational fusions were performed to attach FBN1b or the different fragments of AtSS4 to the N terminus of YFP (pXNGW-(*n*YFP)) or the C terminus of cyan fluorescent protein (CFP, pXCGW-(*c*CFP)) for bimolecular fluorescence complementation (BiFC) assays (13). An overlapping PCR strategy was employed to clone fragments C, D, and CR to fuse the AtSS4 chloroplast transit peptide (CTP) with the sequence of interest and to clone the AtSS4 protein without the conserved region (CR, AtSS4_WOCR) (see the oligos in supplemental Table S1). In the case of AtSS4_WOCR, 135 bp (from 1411 to 1545 bp of the AtSS4 cDNA sequence) were eliminated. The procedures for cloning cDNAs encoding FBN1b, the full-length SS4 protein, and its N- and C-terminal segments were described previously (11).

The complete cDNA of the *Brachypodium dystachion* SS4 (BdSS4) (Bradi2g18810.1) was synthesized from the total RNA extracted from seeds. The primers were designed to contain the attB sequences (supplemental Table S1) compatible with the Gateway system. The stop codon was eliminated to allow further C-terminal translational fusions. The sequenced PCR product was cloned into pDNOR207 (Invitrogen) via the BP clonase reaction. The sequence was then cloned into different pEntry vectors via LR reactions. The binary vector pCTAPi (14) was used to transform the *Arabidopsis ss4* mutant. pEarleyGate 103 (12), which allows fusion with GFP, was used to localize the

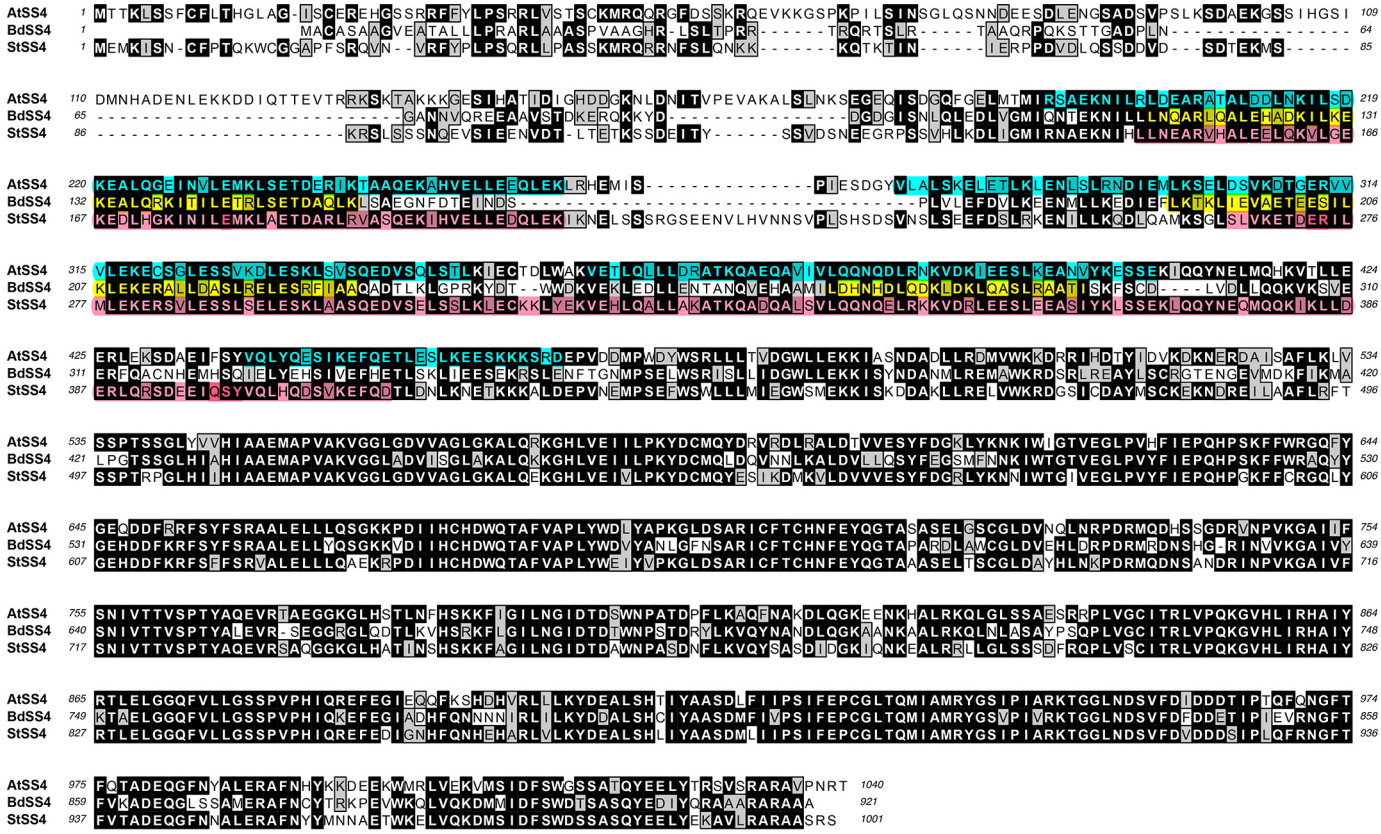

FIGURE 3. **Sequence alignment of amino acids in SS4 proteins from *A. thaliana* (AtSS4), *B. distachyon* (BdSS4), and *S. tuberosum* (StSS4).** Coiled-coil regions predicted by the MULTICOIL program are indicated in *blue*, *yellow*, and *red*, respectively. Identical amino acids are enclosed in *black boxes*. Conserved substitutions are enclosed in *gray boxes*. The alignment was performed by the MacVector program.

fusion protein *in vivo*, and pXNGW and pXCGW (13) were used for BiFC assays.

The cDNA fragments encoding AtSS4 and its truncated versions without the CTP (fragments A, B, C, D, and E and the C terminus; see schematic in Fig. 11) were amplified by PCR (supplemental Table S1) and inserted into the pET45b(+) expression vector (Novagen) at the BamHI-XhoI sites. The cDNA fragment encoding the AtSS4 protein without the CR and CTP was cloned into the pDON207 vector via a BP clonase reaction and then transferred to the pDEST17 vector via an LR clonase reaction. Both the pET45b(+) and pDEST17 vectors introduce a His_5 tail at the N terminus of the cloned fragments. Recombinant clones were transformed into Δ*glg*CAP BL21 (DE3) *Escherichia coli* cells lacking endogenous GS activity (15).

Arabidopsis Transformation and Selection—The binary vector pCTAPi (14) containing the complete BdSS4 cDNA was introduced into the *Agrobacterium tumefaciens* C58 strain and used to transform the *Arabidopsis ss4*-1 mutant (9) via the floral dip method (16). The transformed plants were selected for their herbicide (BASTA) resistance. Transgene expression was analyzed in 19 resistant plants selected by quantitative real-time RT-PCR analysis using specific primers for the BdSS4 sequence. Total RNA was isolated from *Arabidopsis* leaves using TRIsure reagents (Bioline Ltd., London, UK) according to the instructions of the manufacturer. First-strand cDNA synthesis and quantitative real-time PCR assays were performed as described previously (17). The specific primers used for amplifying BdSS4 were BdSS4_qRTPCR_F (5′-CCGACCCACTTAATGGGGCTAAT-3′) and BdSS4_qRTPCR_R (5′-GCATGTTCCAATGCCTGAAGACG-3′). The primers used amplify UBQ10, a housekeeping gene, were UBQF (5′-GATCTTTGCCGGAAAACAATTGGAGGATGGT-3′) and UBQR (5′-CGACTTGTCATTAGAAAGAAAGAGATAACAG-3′). Three transgenic *Arabidopsis* lines with different levels of BdSS4 expression (line 16 with low levels and lines 17 and 19 with high levels) were selected for further characterization.

Transient Expression in N. benthamiana—Corresponding transgene vectors were electroporated into *A. tumefaciens* strain C58 (18). The agroinfiltration of *N. benthamiana* leaves was assessed as described previously (11).

Confocal Microscopy—A DM6000 confocal laser-scanning microscope (Leica Microsystems) equipped with a ×63 oil immersion objective and a ×20 objective was used to detect protein localization based on GFP fusion expression or protein-protein interaction in BiFC assays performed in *N. benthamiana* mesophyll cells. GFP or YFP/CFP expression and chlorophyll autofluorescence imaging was performed by exciting the cells with an argon laser at 488 nm and detecting fluorescence emissions at 500–525 nm and 630–690 nm, respectively.

Bacterial Expression—Aliquots of overnight cultures (0.5 ml) were transferred to 50 ml Luria-Bertani medium containing 50 μg/ml ampicillin and 100 μg/ml kanamycin. Cultures were incubated at 25 °C until they reached an optical density of 0.5 at 600 nm. Cultures were induced to express SS4 polypeptides by adding 1 mM isopropyl-1-thio-β-D-galactopyranoside at 25 °C for 90 min. Bacterial cells from induced cultures were harvested

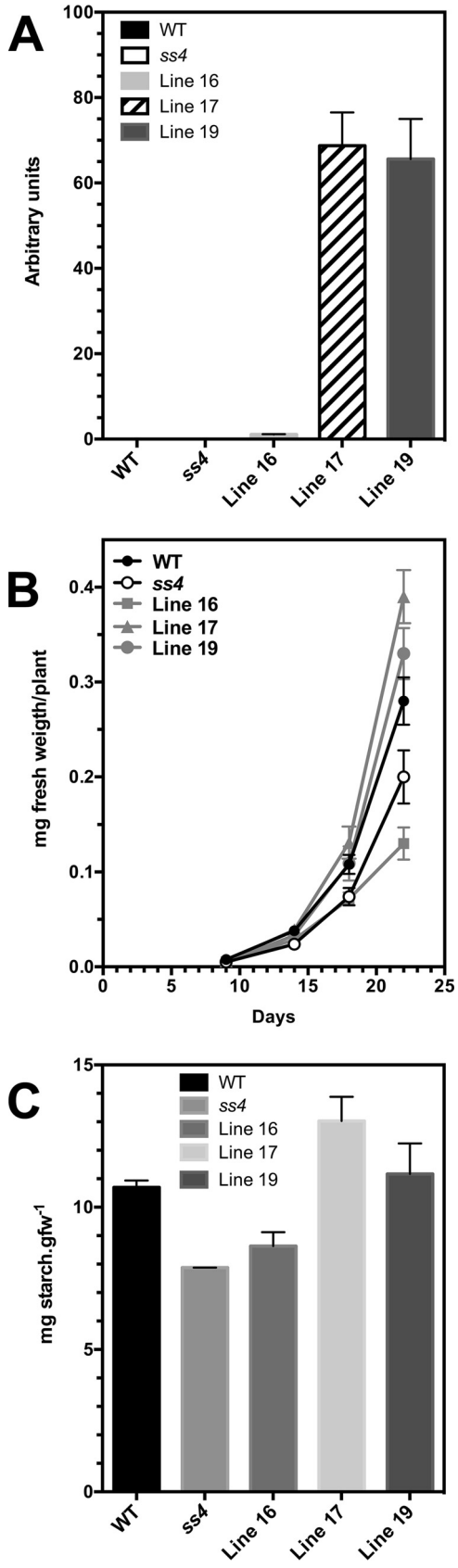

FIGURE 4. **Complementation of the *Arabidopsis ss4-1* mutant with the *Brachypodium* SS4 protein.** cDNA encoding the *Brachypodium* SS4 full-length protein was expressed in the *Arabidopsis ss4-1* mutant under a ^{35}S constitutive promoter. *A*, expression of the *Brachypodium* SS4 gene in *Arabidopsis* WT and the *ss4*-1 mutant (*ss4*) and in three transgenic lines (lines 16, 17, and 19). Values represent the mean ± S.D. of four independent experiments. *B*, growth of plants described in *A*. Growth was estimated by weighing the aerial part of the plants. Values represent the mean ± S.D. of three independent experiments. *C*, starch accumulation at the end of the day period in plants described in *A* grown under a 16-h light/8-h dark photoregime. Values represent the mean ± S.D. of three independent experiments.

by centrifugation, washed with 50 mM Hepes (pH 8.0), and resuspended in 100 mM Tricine buffer (pH 8.0), supplemented with 1 mM phenylmethylsulfonyl fluoride and 5 μl/ml protease inhibitor mixture (Sigma-Aldrich). Cells were sonicated (Branson digital sonifier, 90 s, 20% intensity, 4 °C) and then centrifuged for 30 min at 20,000 × *g* at 4 °C. The supernatant constituted the crude extract.

Starch Synthase Activity—The reaction was performed in a final volume of 200 μl containing 100 mM Tricine (pH 8.0), 25 mM potassium acetate, 5 mM EDTA, 5 mM DTT, 0.5 mg/ml BSA, 0.5 M sodium citrate, 10 mg/ml amylopectin, and 5 mM ADP-glucose. The reaction was initiated by adding 10 μl of *E. coli* crude extracts obtained as described above. At 0 min (t0), 100 μl of the reaction was boiled for 10 min to stop the reaction. The rest of the assay was incubated at 30 °C for 10 min, and the reaction was stopped by boiling for 10 min. The ADP produced in the reaction was determined by HPLC using a Partisil 10 SAX column and a photodiode array detector.

Starch Determination—The starch content of *Arabidopsis* leaves was determined as described by Szydlowski *et al.* (19).

In Vitro Pulldown Assay—The pET45b(+) and pDEST15 vectors containing the SS4-D fragment and plasmid pGEX-4T2, which allows the expression of GST protein, were transformed into *E. coli* strain BL21 (Invitrogen). The *in vitro* pull-down assay was performed as described previously (11).

Size Exclusion Chromatography—The SS4-C and E fragments were expressed in *E. coli* cells as described above. An aliquot of the crude protein extract (200 μl) was analyzed using a Superose 6 10/300GL column (GE Healthcare) equilibrated with 50 mM phosphate buffer and 0.15 M NaCl (pH 7.0) on an ÄKTA Purifier chromatography system (Amersham Biosciences) at a flow rate of 0.5 ml/min. Fractions of 0.5 ml were recollected and analyzed on immunoblots probed with an anti-His_5 antibody(Penta His HRP-conjugated kit, Qiagen). To determine the apparent molecular weight of the SS4-C and SS4-E fragments, a calibration curve was created by injecting 0.5 ml of gel filtration standard (Bio-Rad), under the same conditions as above and determining the elution volumes of the markers.

Results

SS4 Interacts with Fibrillins 1 through Its Long Coiled-coil Domains—We previously described an interaction between the N-terminal part of SS4 (NtSS4) and FBN1 (11). The N-terminal fragment contains two well differentiated regions. The first region includes four long coiled-coil domains predicted by the MultiCoil program that comprise residues 194–260, 275–347, 358–407, and 438–465 of *Arabidopsis* SS4 (see schematic in Fig. 1). The second region comprises a highly conserved sequence among all SS4 proteins sequenced to date. This CR does not form a coiled-coil

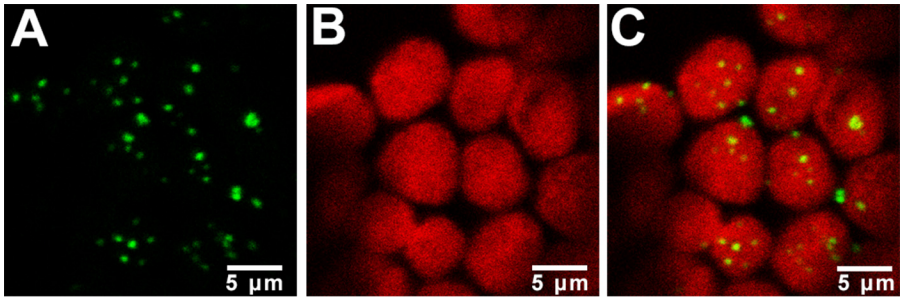

FIGURE 5. **Localization of the *Brachypodium* SS4 protein fused to GFP in *N. benthamiana* chloroplasts.** *A*, GFP fluorescence (*green*). *B*, chlorophyll autofluorescence (*red*). *C*, merged image of *A* and *B*. cDNA encoding the full-length BdSS4 sequence was fused to a GFP sequence and transiently expressed in *N. benthamiana* leaves.

structure. It extends from amino acids 471–515 of *Arabidopsis* SS4. To define the specific region of SS4 involved in the interaction with FBN1, we transiently co-transformed different truncated versions of YFP-tagged NtSS4 and CFP-tagged FBN1b into *N. benthamiana* leaves and analyzed the possible interactions using BiFC assays. First, we found that elimination of the CR (fragment 1) did not affect the interaction between SS4 and FBN1b. Thus, CR was not involved in the interaction between these two proteins (Fig. 1, *A–C*). A SS4 fragment containing the two first coiled-coil domains (CC1 and CC2, fragment 2) could interact with FBN1b (Fig. 1, *D–F*), but subsequent elimination of CC2 (fragment 3) abolished the interaction with FBN1b (Fig. 1, *G–I*). This analysis indicated that the interaction between SS4 and FBN1 required the long coiled-coil domains in the N-terminal part of SS4 and that the CR was not involved in this interaction.

Long Coiled-coil Domains Determine the Localization Pattern of SS4—*Arabidopsis* SS4 is not soluble in the stroma of the chloroplast. Instead, it is located at specific spots associated with the thylakoid membranes (11, 19), most likely because of its interaction with FBN1s proteins, which are localized on the surface of the plastoglobules. To ascertain the involvement of the long coiled-coil region in the localization pattern of SS4, we fused fragments 1, 2, and 3 to GFP and analyzed their pattern of localization in transiently transformed *N. benthamiana* leaves. Eliminating the CR did not affect the localization pattern determined previously for the full-length SS4 protein or NtSS4 fragment (Fig. 2, *A–C*). Eliminating CC3 and CC4 modified the localization pattern of the fused protein. It was detected both as specific spots and in soluble form in the plastidial stroma (Fig. 2, *D–F*). Finally, eliminating CC2, CC3, and CC4 completely modified the localization pattern of the fused protein because it was detected in soluble form in the stroma (Fig. 2, *G–I*). These data indicated that the coiled-coil domains present in the N-terminal part of the protein determined the localization pattern of SS4.

The Functionality of Coiled-coil Domains Is Conserved in Other SS4 Enzymes—Coiled-coil domains are also predicted in SS4 proteins from other plant sources, such as *Solanum tuberosum* and *B. distachyon* (Fig. 3). However, the degree of sequence conservation in these domains is lower than that observed in the C-terminal part of the proteins. To determine whether the SS4 from a phylogenetically distant species, such as *Brachypodium*, can complement the *ss4* mutation in *Arabidopsis*, we cloned the cDNA encoding the full-length *Brachypodium* SS4 protein and transformed it into the *ss4-1 Arabidopsis* mutant lacking the SS4 protein (9). We selected two lines with high levels of *Brachypodium* SS4 expression (lines 17 and 19 in Fig. 4*A*) and one line with negligible levels of *Brachypodium* SS4 expression (line 16). Fig. 4 shows that the *ss4* mutation was complemented successfully in lines 17 and 19. These lines reverted the low growth rate (Fig. 4*B*) and low starch accumulation levels (Fig. 4*C*) observed in the *ss4* mutant plants. In addition, the *Brachypodium* SS4 expression pattern in *Nicotiana* leaves was the same as observed for the *Arabidopsis* protein (Fig. 5). These data indicate that the *Brachypodium* SS4 protein could function in *Arabidopsis*. Thus, the coiled-coil domain functions were conserved in both proteins.

In Vivo SS4-SS4 Interaction—One feature of the coiled-coil domains is the ability to form dimers (or oligomers) (20). Therefore, we analyzed whether one SS4 polypeptide could interact with another SS4 polypeptide *in vivo*. The BiFC assay of transiently transformed *N. benthamiana* leaves showed that SS4 interacted with other SS4 polypeptides (Fig. 6, *A–C*). This interaction seems to be common in SS4 proteins from other species because we also observed interactions between *Brachypodium* SS4 polypeptides in *Nicotiana* leaves (Fig. 7). This interaction also occurred between a full-length SS4 polypeptide and the NtSS4 fragment (from Met^{1} to Tyr^{543} and containing the coiled-coil domains and the CR; Fig. 6, *D–F*) but not with the C terminus of SS4 (CtSS4, from Val^{544} to the end; Fig. 6, *G–I*). We also observed an interaction between two NtSS4 fragments (Fig. 6, *J–L*) but not between NtSS4 and CtSS4 (Fig. 6, *M–O*). These results indicate that the N terminus of SS4 was sufficient for the interaction observed between two SS4 polypeptides.

The CR Is Involved in the SS4-SS4 Interaction—We investigated whether the coiled-coil domains involved in the interaction with FBN1 are also involved in the SS4-SS4 interaction. Different fragments of the SS4 polypeptide (Fig. 8) were used in BiFC assays in *N. benthamiana* leaves. Eliminating CC1 and CC2 (fragment C), which were required for the SS4-FBN1 interaction, did not affect the SS4-SS4 interaction (Fig. 8, *D–F*). This interaction was also observed when the remaining CC3 and CC4 domains were eliminated (Fig. 8, *G–I*), resulting in a fragment with only the CR and the C-terminal part of SS4 (Fig. 8, *fragment D*). On the other hand, eliminating the CR prevented the SS4-SS4 interaction in *Nicotiana* chloroplasts. Fig. 9

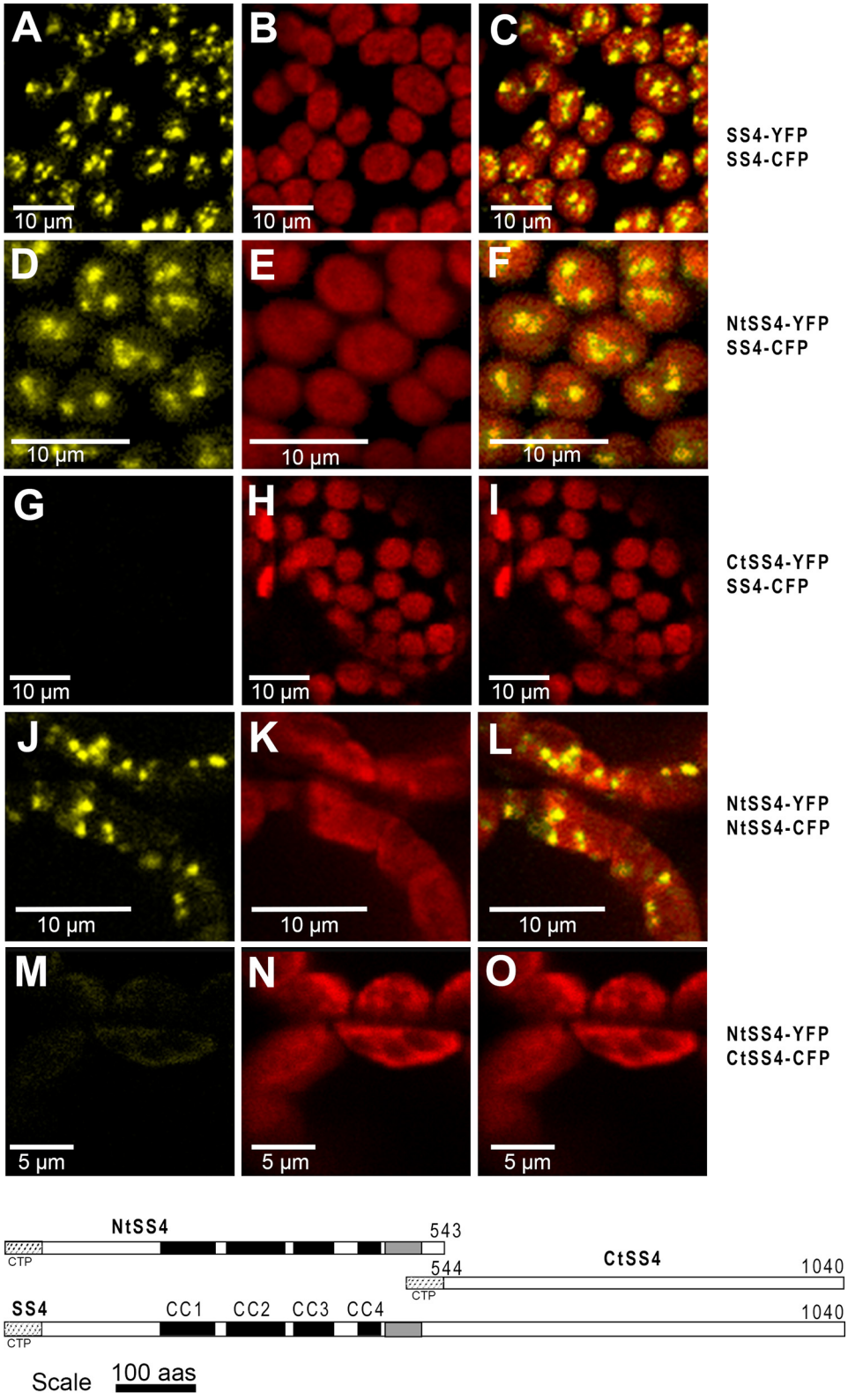

FIGURE 6. **SS4-SS4 interaction *in vivo*.** Fluorescence images showing YFP/CFP fluorescence (*left panels*, *yellow*), chlorophyll autofluorescence (*center panels*, *red*), and merged images of YFP/CFP and chlorophyll fluorescence (*right panels*) in *N. benthamiana* leaves. Leaves were co-transformed with a cDNA encoding the full-length *Arabidopsis* SS4 protein (*A–C*), its N terminus (*D–F* and *J–L*), or its C terminus (*G–I* and *M–O*) fused to the N-terminal half of YFP and the cDNA encoding the full-length SS4 protein (*A–I*) or the N terminus of SS4 (*J–O*) fused to the C-terminal moiety of CFP. The *yellow* signal indicates an interaction between two SS4s or two SS4 fragments. *Bottom panel*, the *Arabidopsis* SS4 protein and the N- and C-terminal polypeptides. *Black boxes* correspond to coiled-coil regions. The *gray box* indicates the CR found in SS4 proteins. The *dotted box* indicates the CTP of the SS4 protein. The numbers indicate the positions of the respective amino acid residues (*aas*). The combination of polypeptides used in each case is indicated beside the respective panels.

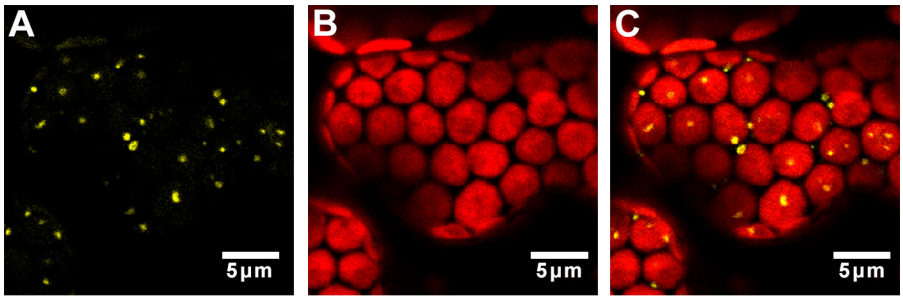

FIGURE 7. **Brachypodium SS4-SS4 interaction *in vivo*.** Two plasmids were constructed with cDNAs encoding the full-length *Brachypodium* SS4 protein fused to either the N-terminal half of YFP or the C-terminal half of CFP. Both plasmids were co-transformed and transiently expressed in *N. benthamiana* chloroplasts. *A*, YFP/CFP fluorescence (*yellow*). *B*, chlorophyll autofluorescence (*red*). *C*, merged images of *A* and *B*. The *yellow* signal indicates an interaction between two SS4 polypeptides.

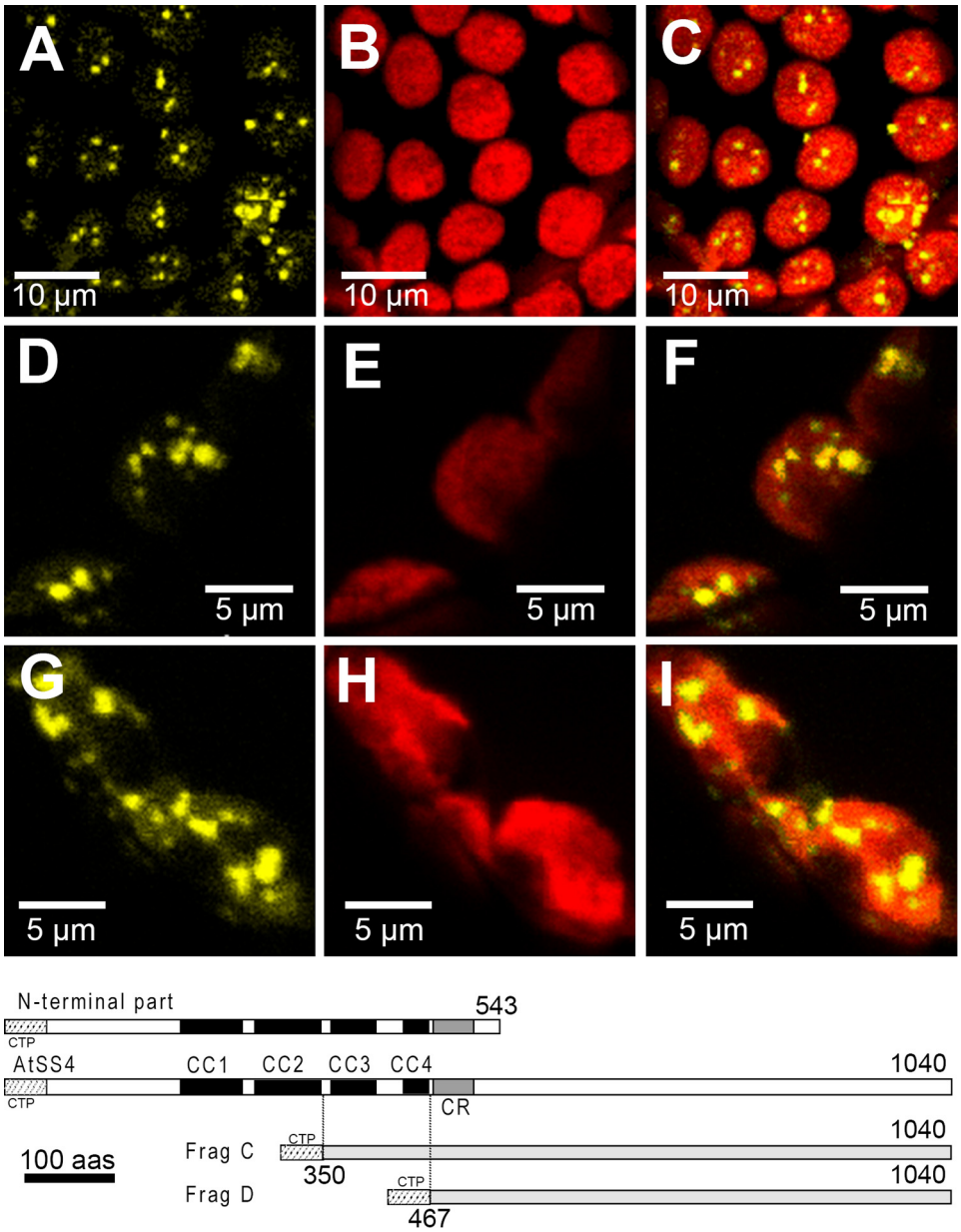

FIGURE 8. **SS4-SS4 interaction *in vivo*.** *Top panels*, fluorescence images showing YFP/CFP fluorescence (*left panels*, *yellow*), chlorophyll autofluorescence (*center panels*, *red*), and merged images of YFP/CFP and chlorophyll fluorescence (*right panels*) in *N. benthamiana* leaves. Leaves were co-transformed with a cDNA encoding the N terminus of *Arabidopsis* SS4 protein (*A–C*), fragment C (*D–F*), or fragment D (*G–I*) fused to the N-terminal half of YFP and the cDNA encoding the full-length SS4 protein fused to the C-terminal part of CFP. The *yellow* signal indicates an interaction between the two SS4s or SS4 and an SS4 fragment. *Bottom panel*, schematic showing the *Arabidopsis* SS4 protein and the positions of fragments (*Frag*) C and D in the protein. *Black boxes* correspond to coiled-coil regions. The *gray box* indicates the highly conserved region found in various SS4 proteins. The *dotted box* indicates the CTP of the SS4 protein. The numbers indicate the positions of the respective amino acid residues (*aas*).

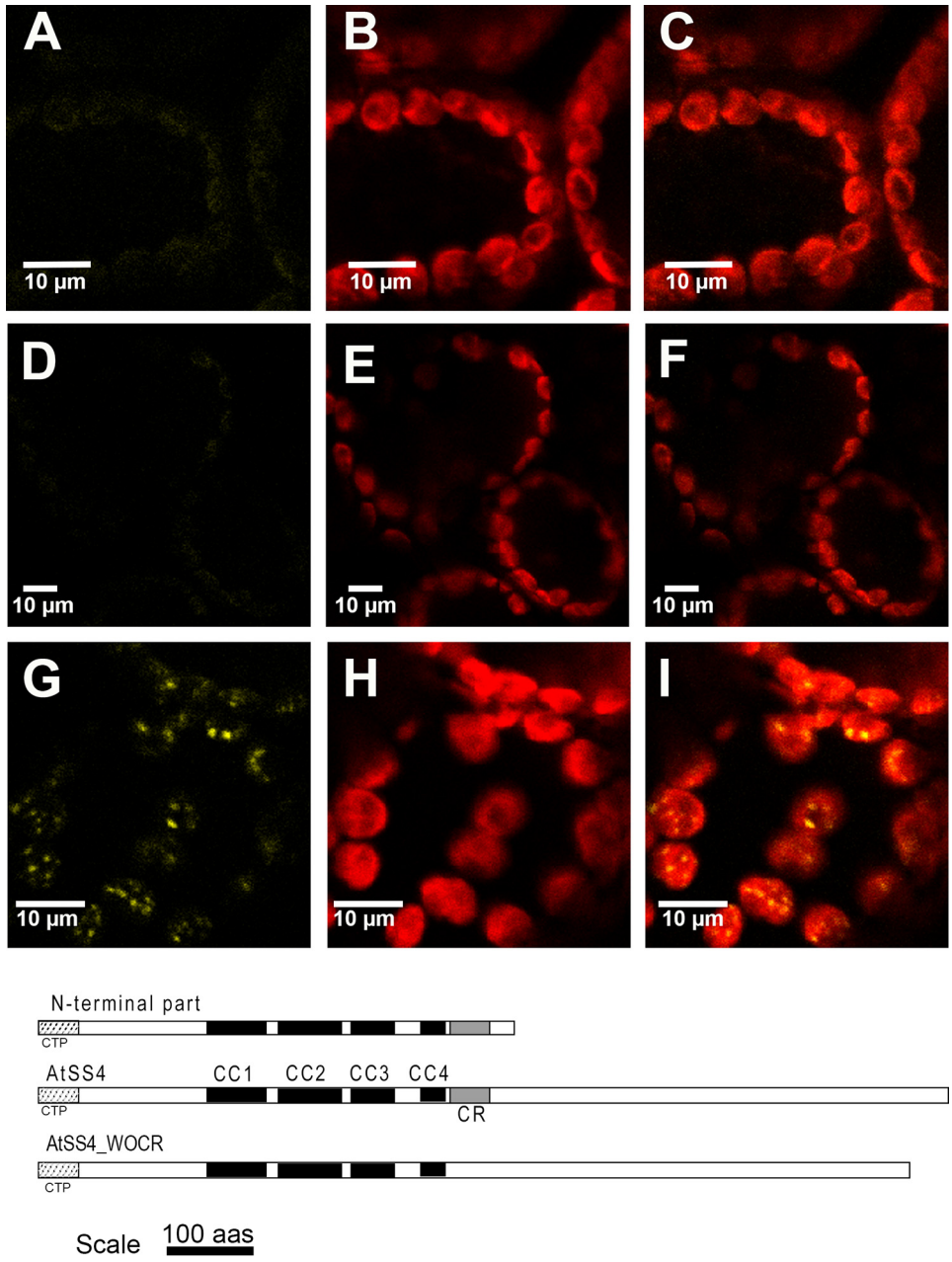

FIGURE 9. **Effect of the elimination of the CR on the SS4-SS4 interaction *in vivo*.** *Top panels*, fluorescence images showing YFP/CFP fluorescence (*left panels*, *yellow*), chlorophyll autofluorescence (*center panels*, *red*), and merged images of YFP/CFP and chlorophyll fluorescence (*right panels*) in *N. benthamiana* leaves. Leaves were co-transformed with a cDNA encoding the full-length SS4 protein without the CR (*A–F*) or the full-length SS4 polypeptide (*G–I*) fused to the N-terminal half of YFP and the cDNAs encoding the full-length SS4 protein (*A–C* and *G–I*) or the N-terminal part of SS4 (*D--F*) fused to the C-terminal part of CFP. The *yellow* signal indicates an interaction between SS4 polypeptides. *Bottom panel*, schematic showing the *Arabidopsis* SS4 (*AtSS4*), the N-terminal part of SS4, and the SS4 polypeptide without the CR (*AtSS4_WOCR*). *Black boxes* correspond to coiled-coil regions. The *gray box* indicates the CR. The *dotted box* indicates the CTP of the SS4 protein. *aas*, amino acid residues.

shows that the AtSS4 protein lacking the CR (AtSS4_WOCR) did not interact with the full-length SS4 protein (Fig. 9, *A–C*) or the N-terminal part of SS4 (Fig. 9, *D–F*). We also expressed the CR in *Nicotiana* leaves but observed that the levels were very low. Thus, the BiFC assays performed to investigate the interaction between the CR alone and the SS4 polypeptide did not show clear results (data not shown).

The ability of fragment D to interact with another fragment D polypeptide was also tested in a pulldown assay with polypeptides expressed in *E. coli*. GST-tagged fragment D was successfully co-purified with His-tagged fragment D (Fig. 10), indicating that both polypeptides interacted *in vitro*. These results suggest that the CR mediates the SS4-SS4 interaction but that the coiled-coil domains were not involved.

SS4 Forms a Dimer—The BiFC assays used to study the SS4-SS4 interaction did not indicate whether SS4 formed a dimer or any other oligomer *in vivo*. To address this question, we expressed SS4 in *E. coli* and analyzed the apparent molecular weights of the purified proteins in size exclusion chromatography on a Superose 6 (GE Healthcare) gel. When SS4 was expressed in *E. coli*, it was subjected to proteolysis, resulting in protein fragments of different sizes (Fig. 11). This hindered

the use of chromatography for determining the size of the SS4 complex because different peaks were obtained with protein elution. Therefore, we analyzed the expression profiles of different truncated versions of SS4 (see the fragments in Fig. 11). Fragment C displayed a single band when extracted from *E. coli* and was selected for further analyses. Fig. 12 shows a representative elution profile of crude *E. coli* extracts. Because fragment C was tagged with a His_5 tail, it could be analyzed by immunoblotting with anti-His_5 antibody (Fig. 12*A*), and the bands were quantified (Fig. 12*B*). The peak (fraction 23) was eluted in 15.23 ml, corresponding to a K_{av} of 0.459, indicating a molecular weight of 167,880 based on the calibration curve created with protein standards (Fig. 12*C*). This M_r was twice (×2.12) the size of fragment C (M_r = 79,000), which suggested that SS4 formed a dimer *in vivo*. A similar study was performed with fragment E (see schematic in Fig. 11), which lacks the coiled-coil domains and the CR and has an M_r of 59,290. The elution peak of *E. coli* extract containing fragment E gave a K_{av} of 0.5833, which corresponded to an M_r of 50,118. These results suggest that fragment E is a monomer *in vivo* and support the idea that the CR is necessary for the dimerization of SS4.

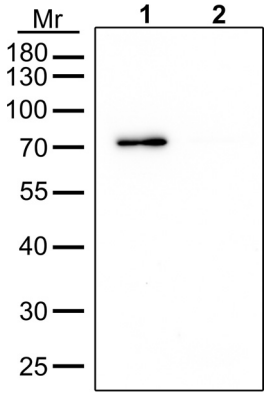

FIGURE 10. **SDS-PAGE analysis of fragment D isolated *in vitro* by a pull-down assay.** *E. coli* extracts containing recombinant protein, fragment D-GST (fragment D of *Arabidopsis* SS4, shown in Fig. 7, fused to GST) or fragment D-His_5 were incubated with glutathione-Sepharose beads. After washing, the proteins bound to the beads were analyzed by SDS-PAGE. The resulting immunoblot was probed with an antibody against His_5. *Lane 1*, extracts that contained fragments D-GST and D-His_5; *lane 2*, extracts containing GST and fragment D-His_5. The molecular weights of the protein markers are indicated.

Dimerization Is Necessary for SS4 Activity—We analyzed the effect of dimerization on the activity of SS4 by expressing the full-length SS4 protein and SS4 polypeptide lacking the CR (a deletion from Met^{471} to Tyr^{515}, see Fig. 13) in an *E. coli* strain lacking endogenous GS activity (15). The expression levels of the non-degraded form of both polypeptides were equivalent, as determined by immunoblot using anti-His_5 antibody (data not shown). Using amylopectin as a primer, the AtSS4 protein had an activity of 7.73 ± 1.44 (S.D.) nmol·min^{-1}, whereas the activity of the polypeptide lacking the CR was 0.13 ± 0.04 nmol·min^{-1} (n = 5 in both determinations). These results indicate that preventing the formation of a dimer drastically reduced the activity of SS4 and suggests that dimerization is necessary for the activity of the enzyme.

Dimerization Is Necessary for the SS4-Fibrillins 1 Interaction—Finally, we investigated which form (dimer or monomer) of SS4 interacts with fibrillins 1. The cDNA coding for the SS4 polypeptide lacking the CR was cloned into the pXNGW-

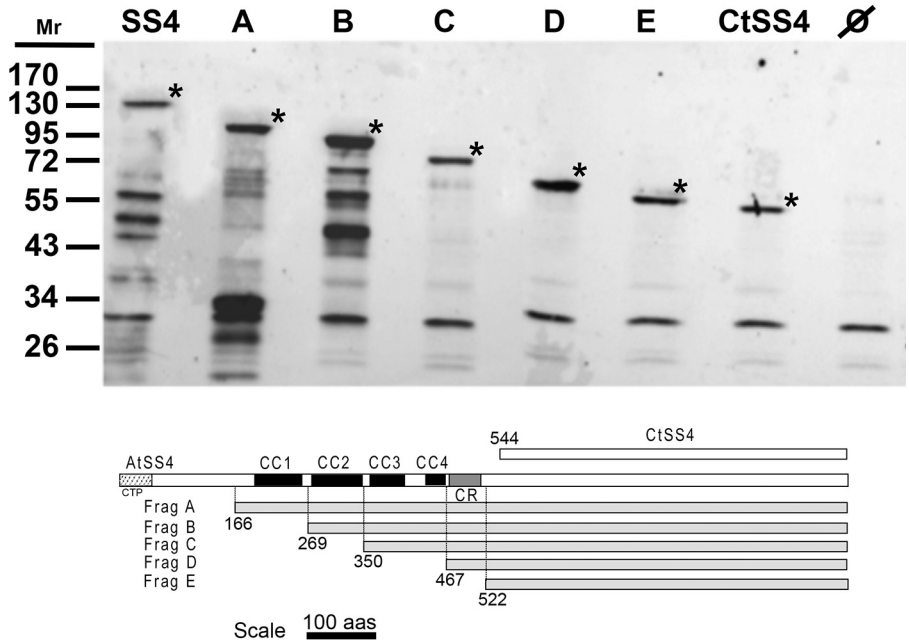

FIGURE 11. **Immunoblot analysis of different SS4 fragments expressed in *E. coli*.** *Top panel*, immunoblot showing the purification of different truncated versions of AtSS4 tagged with a His_5 tail that were expressed in *E. coli*. Cells were disrupted by sonication and centrifuged. The supernatant (10 μl) was analyzed on immunoblots probed with anti-His_5. *SS4*, full-length AtSS4 without the chloroplast transit peptide; *A–E*, SS4 fragments A–E (see *bottom panel*); *CtSS4*, C terminus of AtSS4. Ø, empty expression vector. *Asterisks* indicate the bands that correspond to the molecular weights predicted for the respective constructs. The molecular weights of the protein markers are indicated. *Bottom panel*, schematic showing the *Arabidopsis* SS4 protein and the positions of fragments (*Frag*) A–E and CtSS4. *Black boxes* correspond to coiled-coil regions. The *gray box* indicates the highly conserved region found in SS4 proteins. The *dotted box* indicates the CTP of the SS4 protein. *aas*, amino acid residues.

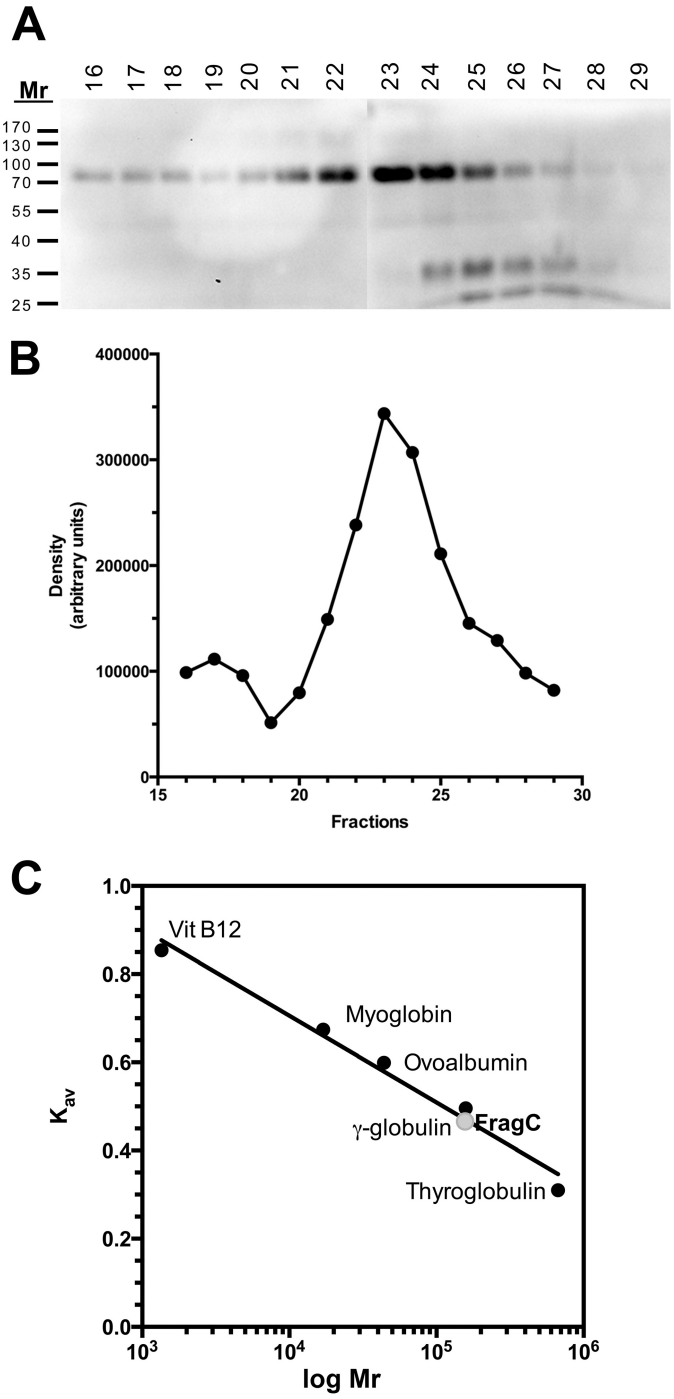

FIGURE 12. **Size exclusion chromatography of AtSS4 fragment C.** Crude extract of *E. coli* containing *Arabidopsis* SS4 fragment C was loaded onto a Superose 6 column. 0.5-ml fractions were collected, analyzed by immunoblot electrophoresis, and probed with the anti His_5 antibody. *A*, immunoblot for fractions 16–29. The molecular weights of the protein markers are indicated. *B*, the densities of the bands in *A*, quantified by Quantity One software (Bio-Rad). *C*, K_{av} (elution volume − column void volume (7.80 ml in this case)/total bed volume (24 ml in this case) − column void volume) *versus* the logarithm of the molecular weights (*MW*) of different polypeptides, which were used as size markers in the chromatography. The position of fragment C in the curve is indicated by a *gray dot*. *Frag*, fragment; *Vit*, vitamin.

(*n*YFP) vector to fuse the polypeptide to the N-terminal part of YFP. It was then co-transformed with FBN1b fused to the C-terminal part of CFP into *Nicotiana* leaves. The SS4 polypeptide lacking the CR is unable to interact with FBN1b (Fig. 14, *A–C*). These results suggest that fibrillins 1 interacts *in vivo* with the dimerized form of SS4.

Discussion

Initiation of the starch granule remains an uncharacterized process, but our group has demonstrated that SS4 is involved in this process. SS4 controls the number of starch granules that accumulate in chloroplasts, and it is involved in the initiation of starch granules (9, 21). The interaction between SS4 and fibrillin 1 proteins (plastoglobule-associated proteins) has been suggested to mediate protein localization to the thylakoid membranes (11). In this study, we showed that the SS4-FBN1s interaction occurred through the coiled-coil domains situated within the N-terminal part of SS4 (Fig. 1). In addition, these domains were responsible for the dot-like localization pattern of SS4 (Fig. 2). The coiled-coil domain is a characteristic feature of SS4 and has been found in the N-terminal part of SS4s from other plant sources that are phylogenetically distant, such as *S. tuberosum* and *B. distachyon* (Fig. 3). This N-terminal domain sequence was conserved to a lesser degree than the C terminus of SS4s proteins, which was homologous to other SSs and to GS. Thus, the fourth predicted coiled-coil domain found in *Arabidopsis* SS4 was not present in the *Brachypodium* enzyme. However, the functionality of the region seems to be conserved between SS4 proteins from different plant sources because *Brachypodium* SS4 could compensate for the absence of SS4 in an *Arabidopsis* mutant and exhibited the expected expression pattern in *Nicotiana* leaves (Figs. 4 and 5). These results point to a conserved mechanism of action for SS4 in the synthesis of starch for both transitory (*Arabidopsis* leaves) and long-term (*Brachypodium* seeds) storage in plants.

A protein homologous to SS4, GS, acts as a dimer, trimer, or tetramer in eukaryotes (22–25). It forms homodimers in bacteria and a trimer in archaea (26). The crystallized rice granule-bound SSI and *Hordeum vulgare* SS1 were monomers in the crystal, with no significant intermolecular interaction surfaces (27, 28). However, we showed that SS4 interacts with other SS4 polypeptides to form dimers *in vivo* (Figs. 6 and 12). Surprisingly, the long coiled-coil region was not involved in protein dimerization. This process was mediated by a region situated between the coiled-coil region and the glucosyltransferase domain. This region is specific to class 4 SSs, and is not present in GS, but it is highly conserved between all SS4 proteins sequenced to date (Fig. 13). These findings suggest that SS4 dimerization is a common process in different plant species. We confirmed that *Brachypodium* SS4 interacts with other *Brachypodium* SS4 polypeptides (Fig. 7), indicating that the SS4 mechanism of dimerization has been conserved between dicot and monocot plant species.

The dimerization of SS4 appeared to be necessary for its enzymatic activity because elimination of the CR led to a 60-fold reduction in SS4 activity. In addition, the dimerization seemed to be required for the interaction of SS4 with fibrillins 1 (Fig. 14). This result seems to be in discrepancy with the results shown in Fig. 1, where an interaction between FBN1b and an SS4 fragment containing the coiled-coil domains without the CR is shown. We observed that the elimination of the C-termi-

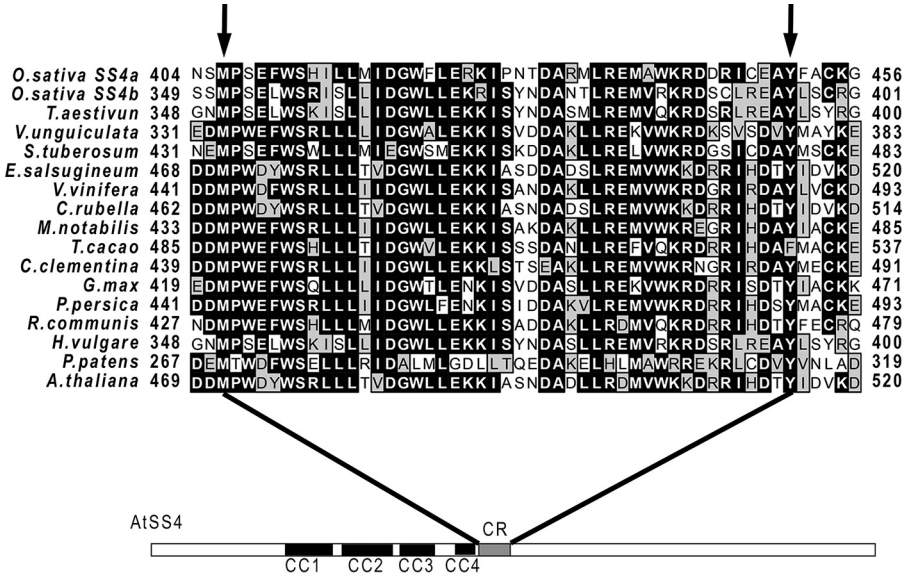

FIGURE 13. **Alignment of the amino acid sequences of the highly conserved region of SS4 proteins from different plant species.** Identical amino acids are indicated by *black boxes*. Conserved substitutions are indicated by *gray boxes*. The alignment was performed using the MacVector program. The *arrows* indicate the start and end points of the CR region considered in this study.

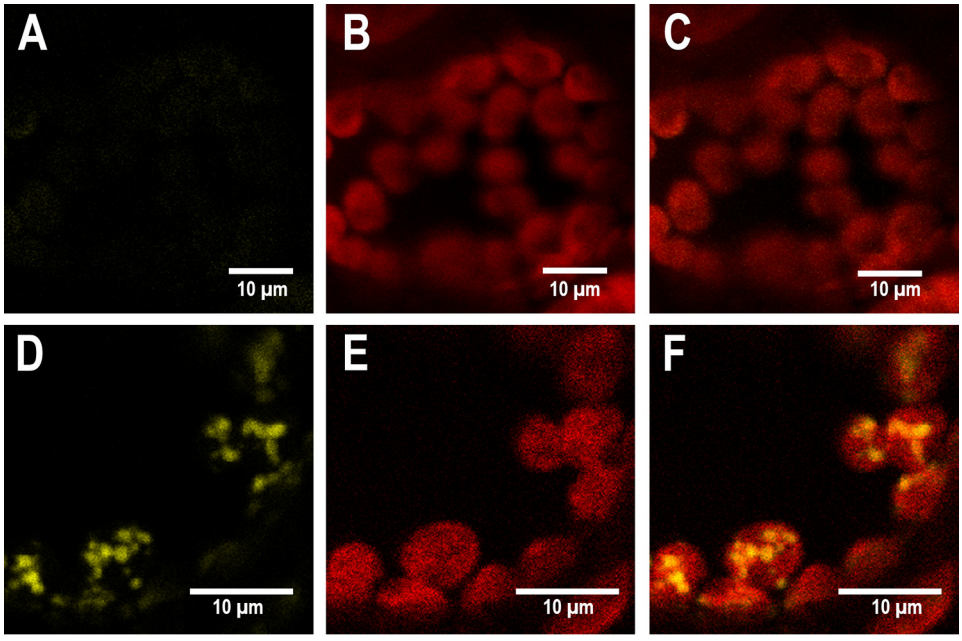

FIGURE 14. **Effect of eliminating the CR on the SS4-FBN1b interaction *in vivo*.** Fluorescence images show YFP/CFP fluorescence (*left panels*, *yellow*), chlorophyll autofluorescence (*center panels*, *red*), and merged images of YFP/CFP and chlorophyll fluorescence (*right panels*) in *N. benthamiana* leaves. Leaves were co-transformed with a cDNA encoding the full-length SS4 protein without the CR (*A–C*) or the full-length SS4 polypeptide (*D–F*) fused to the N-terminal half of YFP and the cDNAs encoding the FBN1b protein fused to the C-terminal part of CFP. The *yellow* signal indicates an interaction between SS4 and FBN1b.

nal part of SS4 considerably increases the intensity of fluorescence detected in the BiFC assay with FBN1b (data not shown), suggesting that the full-length SS4 polypeptide has much less affinity for FBN1b than the N-terminal part of the protein alone. An explanation for the discrepancy observed is that the prevention of forming dimers (by eliminating the CR) would decrease the affinity of SS4_WOCR for FBN1b so that the fluorescence signal cannot be detected in the BiFC assay (Fig. 14). In the case of the N-terminal fragment of SS4, the decrease of affinity promoted by the elimination of the CR would not be enough to avoid detection of the fluorescence signal in the BiFC assay (Fig. 1). It is tempting to speculate that dimerization represents a mechanism that controls the localization and activity of SS4 so that the enzyme is active when just associated to plastoglobules and when its participation in the synthesis of a new starch granule is required. In this respect, it is interesting to note the presence of a Tyr residue in the CR (the last residue in the CR indicated in Fig. 13). This Tyr has been predicted to have a high probability of being phosphorylated (NetPhos2.0.), suggesting that a mechanism of phosphorylation may be involved in controlling the dimerization state of SS4. Further studies are neces-

sary to test this hypothesis and to characterize the function of the SS4 dimerization in starch metabolism.

Author Contributions—A. M. designed the study and wrote the paper. S. R. cloned the *Brachypodium* SS4 gene, transformed it in the *Arabidopsis* mutant, analyzed the transgenic lines, and performed most of the BiFC and GFP experiments. P. R. cloned the different *Arabidopsis* SS4 fragments and expressed them in *E. coli*. T. R. studied the degree of oligomerization of SS4. All authors analyzed the results and approved the final version of the manuscript.

Acknowledgments—We thank Alicia Orea for technical assistance with the confocal microscope analyses.

References

1. Stitt, M., and Zeeman, S. C. (2012) Starch turnover: pathways, regulation and role in growth. *Curr. Opin. Plant Biol.* **15,** 282–292
2. Zeeman, S. C., Kossmann, J., and Smith, A. M. (2010) Starch: its metabolism, evolution, and biotechnological modification in plants. *Annu. Rev. Plant Biol.* **61,** 209–234
3. Santelia, D., and Zeeman, S. C. (2011) Progress in *Arabidopsis* starch research and potential biotechnological applications. *Curr. Opin. Biotech.* **22,** 271–280
4. Seung, D., Soyk, S., Coiro, M., Maier, B. A., Eicke, S., and Zeeman, S. C. (2015) protein targeting to starch is required for localising granule-bound starch synthase to starch granules and for normal amylose synthesis in *Arabidopsis*. *PLoS Biol.* **13,** e1002080
5. Ball, S. G., and Morell, M. K. (2003) From bacterial glycogen to starch: understanding the biogenesis of the plant starch granule. *Annu. Rev. Plant Biol.* **54,** 207–233
6. Leterrier, M., Holappa, L. D., Broglie, K. E., and Beckles, D. (2008) Cloning, characterisation and comparative analysis of a starch synthase IV gene in wheat: functional and evolutionary implications. *BMC Plant Biol.* **8,** 98
7. Imparl-Radosevich, J. M., Keeling, P. L., and Guan, H. (1999) Essential arginine residues in maize starch synthase IIa are involved in both ADP-glucose and primer binding. *FEBS Lett.* **457,** 357–362
8. Imparl-Radosevich, J. M., Li, P., Zhang, L., McKean, A. L., Keeling, P. L., and Guan, H. (1998) Purification and characterization of maize starch synthase I and its truncated forms. *Arch. Biochem. Biophys.* **353,** 64–72
9. Roldán, I., Wattebled, F., Mercedes Lucas, M., Delvallé, D., Planchot, V., Jiménez, S., Pérez, R., Ball, S., D'Hulst, C., and Mérida, A. (2007) The phenotype of soluble starch synthase IV defective mutants of *Arabidopsis thaliana* suggests a novel function of elongation enzymes in the control of starch granule formation. *Plant J.* **49,** 492–504
10. D'Hulst, C., and Mérida, Á. (2012) in *Essential Reviews in Experimental Biology Volume 5: The Synthesis and Breakdown of Starch* (Tetlow, I. J., ed.) pp. 55–76, Society for Experimental Biology, London
11. Gámez-Arjona, F. M., Raynaud, S., Ragel, P., and Mérida, A. (2014) Starch synthase 4 is located in the thylakoid membrane and interacts with plastoglobule-associated proteins in *Arabidopsis*. *Plant J.* **80,** 305–316
12. Earley, K. W., Haag, J. R., Pontes, O., Opper, K., Juehne, T., Song, K., and Pikaard, C. S. (2006) Gateway-compatible vectors for plant functional genomics and proteomics. *Plant J.* **45,** 616–629
13. Yuan, L., Gu, R., Xuan, Y., Smith-Valle, E., Loqué, D., Frommer, W. B., and von Wirén, N. (2013) Allosteric regulation of transport activity by heterotrimerization of *Arabidopsis* ammonium transporter complexes *in vivo*. *Plant Cell* **25,** 974–984
14. Rohila, J. S., Chen, M., Cerny, R., and Fromm, M. E. (2004) Improved tandem affinity purification tag and methods for isolation of protein heterocomplexes from plants. *Plant J.* **38,** 172–181
15. Morán-Zorzano, M. T., Alonso-Casajús, N., Muñoz, F. J., Viale, A. M., Baroja-Fernández, E., Eydallin, G., and Pozueta-Romero, J. (2007) Occurrence of more than one important source of ADPglucose linked to glycogen biosynthesis in *Escherichia coli* and *Salmonella*. *FEBS Lett.* **581,** 4423–4429
16. Clough, S. J., and Bent, A. F. (1998) Floral dip: a simplified method for *Agrobacterium*-mediated transformation of *Arabidopsis thaliana*. *Plant J.* **16,** 735–743
17. Gámez-Arjona, F. M., Li, J., Raynaud, S., Baroja-Fernández, E., Muñoz, F. J., Ovecka, M., Ragel, P., Bahaji, A., Pozueta-Romero, J., and Mérida, Á. (2011) Enhancing the expression of starch synthase class IV results in increased levels of both transitory and long-term storage starch. *Plant Biotechnol. J.* **9,** 1049–1060
18. Wood, D. W., Setubal, J. C., Kaul, R., Monks, D. E., Kitajima, J. P., Okura, V. K., Zhou, Y., Chen, L., Wood, G. E., Almeida, N. F., Jr., Woo, L., Chen, Y., Paulsen, I. T., Eisen, J. A., Karp, P. D., *et al.* (2001) The genome of the natural genetic engineer *Agrobacterium tumefaciens* C58. *Science* **294,** 2317–2323
19. Szydlowski, N., Ragel, P., Raynaud, S., Lucas, M. M., Roldán, I., Montero, M., Muñoz, F. J., Ovecka, M., Bahaji, A., Planchot, V., Pozueta-Romero, J., D'Hulst, C., and Mérida, A. (2009) Starch granule initiation in *Arabidopsis* requires the presence of either class IV or class III starch synthases. *Plant Cell* **21,** 2443–2457
20. Rose, A., and Meier, I. (2004) Scaffolds, levers, rods and springs: diverse cellular functions of long coiled-coil proteins. *Cell Mol. Life Sci.* **61,** 1996–2009
21. D'Hulst, C., and Mérida, A. (2010) The priming of storage glucan synthesis from bacteria to plants: current knowledge and new developments. *New Phytol.* **188,** 13–21
22. Jett, M. F., and Soderling, T. R. (1979) Purification and phosphorylation of rat liver glycogen synthase. *J. Biol. Chem.* **254,** 6739–6745
23. Takeda, Y., Brewer, H. B., Jr., and Larner, J. (1975) Structural studies on rabbit muscle glycogen synthase: I: subunit composition. *J. Biol. Chem.* **250,** 8943–8950
24. Wititsuwannakul, D., and Kim, K. H. (1977) Mechanism of palmityl coenzyme A inhibition of liver glycogen synthase. *J. Biol. Chem.* **252,** 7812–7817
25. Takahara, H., and Matsuda, K. (1978) Biosynthesis of glycogen in *Neurospora crassa*: purification and properties of the UDPglucose:glycogen 4-α-glucosyltransferase. *Biochim. Biophys. Acta.* **522,** 363–374
26. Horcajada, C., Guinovart, J. J., Fita, I., and Ferrer, J. C. (2006) Crystal structure of an archaeal glycogen synthase: insights into oligomerization and substrate binding of eukaryotic glycogen synthases. *J. Biol. Chem.* **281,** 2923–2931
27. Momma, M., and Fujimoto, Z. (2012) Interdomain disulfide bridge in the rice granule bound starch synthase I catalytic domain as elucidated by x-ray structure analysis. *Biosci. Biotechnol. Biochem.* **76,** 1591–1595
28. Cuesta-Seijo, J. A., Nielsen, M. M., Marri, L., Tanaka, H., Beeren, S. R., and Palcic, M. M. (2013) Structure of starch synthase I from barley: insight into regulatory mechanisms of starch synthase activity. *Acta Cryst. Sect. D* **69,** 1013–1025

The N-terminal Part of *Arabidopsis thaliana* Starch Synthase 4 Determines the Localization and Activity of the Enzyme

Sandy Raynaud, Paula Ragel, Tomás Rojas and Ángel Mérida

J. Biol. Chem. 2016, 291:10759-10771.
doi: 10.1074/jbc.M115.698332 originally published online March 11, 2016